

MODE SOFTENING NEAR THE CRITICAL POINT WITHIN EFFECTIVE APPROACHES TO QCD

H. FUJII

Institute of Physics, University of Tokyo, Komaba, Tokyo 153-8902, Japan
E-mail: hfujii@phys.c.u-tokyo.ac.jp

M. OHTANI

Radiation Laboratory, RIKEN, Wako, Saitama 351-0198, Japan
E-mail: ohtani@rarfexp.riken.jp

We study the soft mode along the critical line in the phase diagram with the tricritical point, using the Nambu–Jona-Lasinio model. At the critical point with finite quark mass, the ordering density becomes a linear combination of the scalar, quark number and energy densities, and their susceptibilities diverge with the same exponent. Based on the conservation law, it is argued that the divergent susceptibility of a conserved density must be accompanied by a critically–slowing hydrodynamic mode. The shift of the soft mode from the sigma meson to the hydrodynamic mode occurs at the tricritical point on the critical line.

1. Introduction

The phases of QCD have been explored by investigating the behavior of the quark condensate, the Polyakov loop and the color superconducting gap as functions of the temperature (T) and the quark chemical potential (μ). Among various possibilities on the phase structure, existence of a critical point (CP) as an endpoint of the first–order phase boundary has been theoretically suggested and discussed in the literature^{1,2,3}.

When we extend the phase space by taking the mass (m) of the u and d quarks as the third variable, we can study this CP from the viewpoint of the phase space T – μ – m with a tricritical point (TCP). The static properties of this phase diagram with the TCP is well described by the Ginzburg–Landau (GL) effective potential of the quark condensate σ expanded up to the σ^6 term.⁴ First in the case of exact chiral symmetry $m = 0$ the T – μ plane must be divided into two domains of the symmetric and broken phases with a boundary *line*. Although the order of the singularity of this line is

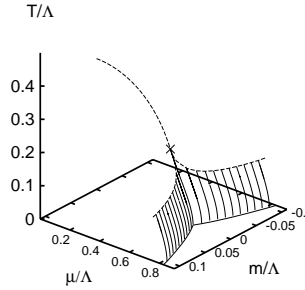


Figure 1. Phase diagram of the NJL model. The critical line is drawn in a dashed line. The first-order phase boundary forms a surface shown by hatch. The TCP is indicated by \times .

unknown in general, we *assume* the TCP where the order of the singularity shifts from the 2nd to the 1st order. Next, when the quark mass takes small but non-zero value, the 2nd order line disappears and the assumed TCP becomes a usual CP (see Fig. 1). In this consideration, the relation of this CP to the chiral symmetry is rather obscure.

Characteristic time scale of the system response becomes infinitely large at a CP, which is known as critical slowing down. The mode whose typical frequency vanishes at the CP is called “soft mode.” In the conventional theory increase of this time scale of a soft mode is related to the divergence of the susceptibility at the CP. The most familiar example will be the sigma meson or the radial fluctuation of the quark condensate in the chiral critical transition⁵.

In this talk we discuss the soft mode along the line of the CP within effective approaches to QCD.^{6,7} We will point out that the soft mode associated with the CP at finite m must have hydrodynamic character. This argument is based on the conservation of the baryon number and energy densities, and therefore is very general. Near the TCP the critical mode is different between the symmetric and broken phases. Although we restrict ourselves to the result obtained in the Nambu–Jona-Lasinio (NJL) model here, we should stress that the same result can be reached within the time-dependent GL approach as well.⁷

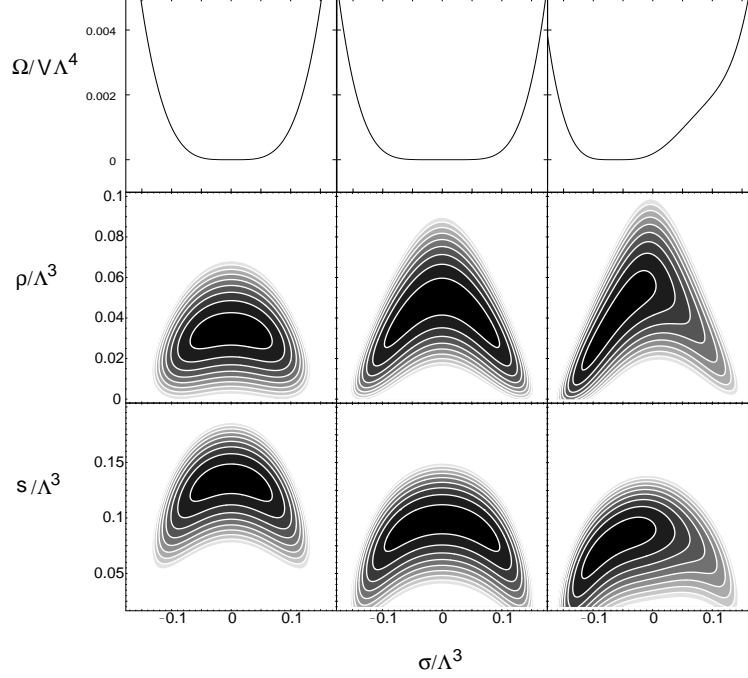


Figure 2. Effective potentials $\tilde{\Omega}$ with two ordering densities, σ - ρ and σ - s at critical points, chiral CP (left), TCP (middle), CP (right). Those with the single ordering density (uppermost) are also shown.

2. Effective potential

We use the NJL model^{8,9} $\mathcal{L} = \bar{q}(i\partial - m)q + g[(\bar{q}q)^2 + (\bar{q}i\gamma_5\tau^a q)^2]$, in the mean field approximation ($\langle\bar{q}q\rangle = \sigma = \text{const}$, $\langle\bar{q}i\gamma_5\tau^a q\rangle = \pi = 0$). The thermodynamics is described by the effective potential,

$$\Omega(T, \mu, m; \sigma)/V = -\nu \int \frac{d^3k}{(2\pi)^3} [E - T \ln(1 - n_+) - T \ln(1 - n_-)] + \frac{1}{4g}(2g\sigma)^2, \quad (1)$$

where $n_{\pm} = (e^{\beta(E \mp \mu)} + 1)^{-1}$, $E = \sqrt{M^2 + \mathbf{k}^2}$, $M = m - 2g\sigma$, and $\nu = 2N_f N_c = 2 \cdot 2 \cdot 3 = 12$ with N_f and N_c the numbers of flavor and color, respectively. The true thermodynamic state is determined by the extremum condition, $\partial\Omega/\partial\sigma = 0$, and the corresponding grand potential is $\Omega(T, \mu, m)$. We define the model with the three-momentum cutoff Λ and with the coupling constant $g\Lambda^2 = 2.5$ which allows the TCP. In the following, all the

dimensionful quantities are expressed in the units of Λ .

It is useful to define the GL effective potential $\tilde{\Omega}$ with two order parameters in studying the true flat direction.⁷ It is numerically constructed as shown in Fig. 2 at the chiral CP with $(T, \mu) = (0.3419, 0.3)$, the TCP $(0.20362, 0.49558)$ and a CP $(0.1498, 0.5701)$ with $m = 0.01$ in the units of Λ .⁶ The susceptibilities $\chi_{ij} = -\frac{1}{V} \partial^2 \Omega / \partial i \partial j$ ($i, j = T, \mu, m$) are equal to the inverse of the curvature matrix of the GL effective potential at the extremum point. Therefore the divergence of the susceptibilities at the critical point is related to the appearance of a flat direction in the GL effective potential.

At the chiral CP, the flat direction must be the scalar density σ due to symmetry (Fig. 2). The susceptibility of σ is divergent while those of the quark number density ρ and the entropy density s remain finite in the mean field approximation.

The σ^2 and σ^4 terms in the potential (1) vanish at the TCP. This fact results in the large fluctuation along the potential valley of $\tilde{\Omega}$ with two ordering densities (Fig. 2). The fluctuations of ρ and s become divergent at the TCP approached from the broken phase.^a If we define a potential of *e.g.*, the quark density ρ by eliminating σ with $\partial \tilde{\Omega}(\sigma, \rho) / \partial \sigma = 0$, we see that the potential is flat on the lower density side of the critical density ρ_t at the TCP.⁷

On the other hand, at the CP with the explicit breaking $m \neq 0$ the proper ordering direction becomes a linear combination of σ , ρ and s (Fig. 2).^{10,7,11} The susceptibilities of these densities diverge with the same exponent since all of them involve a fraction of the critical fluctuation of the proper ordering density. Here the σ direction is no longer special. One may choose equally well any of these densities as the ordering density in the static GL potential.

3. Susceptibility and spectral density

The susceptibility is obtained in the q -limit of the response function, which allows us to express the susceptibility as a sum of the spectral density:

$$\chi_{ij} = \chi_{ij}(0, \mathbf{q} \rightarrow 0) = \lim_{\mathbf{q} \rightarrow 0} \int \frac{d\omega}{2\pi} \frac{2\text{Im}\chi_{ij}(\omega, \mathbf{q})}{\omega}. \quad (i, j = m, \mu, T) \quad (2)$$

From this expression we see that divergence of the susceptibility is caused by spectral enhancement at $\omega = 0$ or mode softening, provided that the

^aNote that the fluctuation of s is a linear combination of those of the quark number density and the energy density.

spectral density $2\text{Im}\chi_{ij}(\omega, \mathbf{q})$ itself is integrable.

At the chiral CP, the divergence of the scalar susceptibility is generated by softening of the sigma meson mode, which is the chiral partner of the pion mode. However, we should recognize that there is no symmetry reason to expect the massless sigma at the CP with explicit symmetry breaking due to $m \neq 0$.

There is a strong constraint on the spectrum in the fluctuations of the conserved quantity: the modes contributing to the susceptibility of a conserved quantity have to be hydrodynamic, that is, the typical frequency must vanish as $\mathbf{q} \rightarrow \mathbf{0}$. Physically this is a consequence of the existence of the current \mathbf{j} such that $\partial_t \rho + \nabla \cdot \mathbf{j} = 0$ for *e.g.*, the quark number density. Using the fact that the conserved density operator is commutative with the total Hamiltonian and the fluctuation–dissipation theorem, we can express the susceptibility in another form,^{8,7}

$$\chi_{ij} = \beta \lim_{\mathbf{q} \rightarrow 0} \int \frac{d\omega}{2\pi} \frac{2\text{Im}\chi_{ij}(\omega, \mathbf{q})}{1 - e^{-\beta\omega}}. \quad (3)$$

These two expressions (2) and (3) coincide with each other if and only if $\lim_{\mathbf{q} \rightarrow 0} 2\text{Im}\chi_{ij}(\omega, \mathbf{q}) = 2\pi\delta(\omega)\omega\chi_{ij}$. Hence, when the susceptibility of a conserved quantity diverges, there must be a hydrodynamic mode which shows critical slowing.

Finally we remark that the ω –limit of the response function $\chi_{ij}(\omega \rightarrow 0, \mathbf{0})$ has no contribution from the hydrodynamic mode spectrum.

4. Soft modes in the NJL model

The response functions in the random phase approximation are written as

$$\chi_{ij}(iq_4, \mathbf{q}) = \Pi_{ij}(iq_4, \mathbf{q}) + \Pi_{im}(iq_4, \mathbf{q}) \frac{1}{1 - 2g\Pi_{mm}(iq_4, \mathbf{q})} 2g\Pi_{mj}(iq_4, \mathbf{q}). \quad (4)$$

Here polarization functions are defined with the imaginary–time quark propagator $\mathcal{S}(\tilde{k}) = 1/(\tilde{k} + M)$ as

$$\Pi_{ij}(iq_4, \mathbf{q}) = - \int \frac{d^3k}{(2\pi)^3} T \sum_{n=-\infty}^{\infty} \text{tr}_{\text{fcD}} \mathcal{S}(\tilde{k}) \Gamma \mathcal{S}(\tilde{k} - q) \Gamma', \quad (5)$$

where $q_4 = 2l\pi T$ ($l \in \mathbb{Z}$), $\tilde{k} = (\mathbf{k}, k_4 + i\mu)$ with $k_4 = -(2n+1)\pi T$, Γ is an appropriate Dirac matrix, and the traces are taken over the flavor, color and Dirac indices. $\Gamma = 1$ for the scalar, $i\gamma_4$ for the baryon number, and

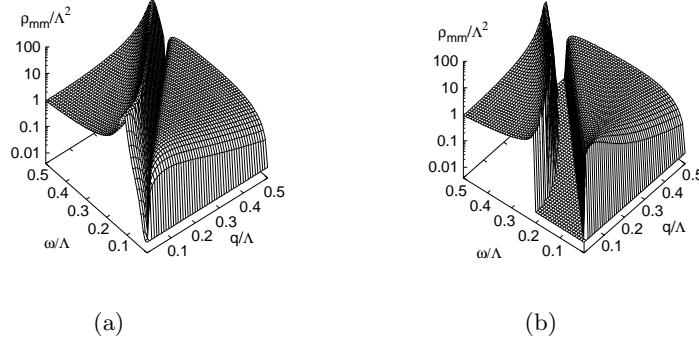


Figure 3. Spectral functions of the scalar channel above (Left, $T/\Lambda = 0.35$) and below (Right, $T/\Lambda = 0.339$) the chiral transition point with $\mu/\Lambda = 0.3$ in the ω - q plane.

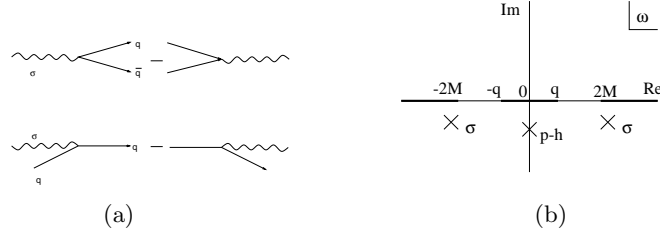


Figure 4. (a) Physical processes contributing to the spectrum with the detailed balance. (b) Analytic structure of the response function. The σ meson and p-h poles (\times) locate in the unphysical Riemann sheet.

\mathcal{H}_{MF} for β with

$$\mathcal{H}_{MF} = -i\frac{1}{2}\vec{\gamma}\cdot\vec{\nabla} + M + i\mu\gamma_4. \quad (6)$$

We deal with the response function of \mathcal{H}_{MF} instead of the entropy because the entropy has no microscopic expression. The real-time response function is obtained from the imaginary-time propagator through the usual replacement $iq_4 \rightarrow q_0 + i\epsilon$ in the final expression.

The collective modes are generated by the infinite sum of the bubble diagrams in the NJL model. The spectral function $\rho_{mm}(\omega, \mathbf{q}) = 2\text{Im}\chi_{mm}(\omega, \mathbf{q})$ of the scalar response function⁵ just above and below the chiral critical point with fixed $\mu = \mu_c$ are shown in Fig. 3. The spectrum in the time-like region comes from the quark pair creation/annihilation while the spectrum in the space-like region is due to the absorption/emission of the scalar fluctuation

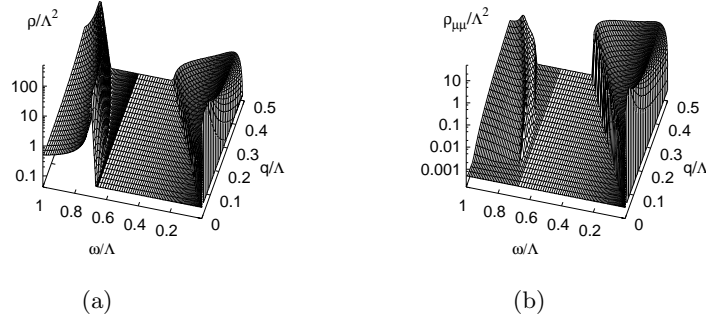


Figure 5. Spectral functions of the scalar and the quark number susceptibilities at the CP with $m/\Lambda = 0.01$.

by a quark or an anti-quark. The latter particle-hole (p-h) process gives rise to the Landau damping of collective motion in medium. These physical processes are schematically shown in Fig. 4 (a). In the unphysical Riemann sheet of ω (Fig. 4 (b)), we found two kinds of complex poles corresponding to the collective excitations of these processes. We shall call here the pole related with the time-like spectrum the sigma meson and the pole for the space-like one the p-h mode.

Approaching the chiral CP from the symmetric phase, we see in Fig. 3 (a) that the sigma meson mode becomes soft. Meanwhile the p-h mode does not show any particular enhancement. From the broken phase, on the other hand, the mass gap of the sigma meson mode is vanishing and the p-h mode spectrum also gets stronger at $\mathbf{q} = \mathbf{0}$ (Fig. 3 (b)).

At the critical point with $m/\Lambda = 0.01$ both the scalar and quark-number susceptibilities diverge. The scalar spectral function is shown in Fig. 5 (a). In this case the sigma meson has finite mass gap, which is set by the quark mass as $\sim 2M \sim m^{1/5}$. The p-h mode has the hydrodynamic character ($\omega \rightarrow 0$ as $\mathbf{q} \rightarrow \mathbf{0}$). We note that the strength of this mode is strongly enhanced at this critical point. In Fig. 5 (b), we show the spectral function of the quark-number response function. It is clear that the divergence is caused solely by the p-h mode spectrum with hydrodynamic character, which is consistent with the general argument given in Sec. 3.

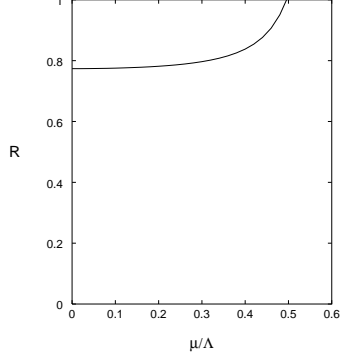


Figure 6. Ratio (7) of the spectral contribution along the chiral critical line in Fig. 1 approached from the broken phase. $R \rightarrow 1$ toward the TCP.

5. Change of the spectral contribution along the critical line

We know that the sigma meson mode is the soft mode associated with the chiral CP while we have seen that the p-h mode shows the critical slowing at the CP with finite quark mass m . Let us study the change of the critical eigenmode along the critical line as shown in a dashed line in Fig. 1, with defining the relative weight of the spectral contributions of the p-h mode to the total spectrum by

$$R \equiv \frac{\chi_{mm}(0, \mathbf{0}^+) - \chi_{mm}(0^+, \mathbf{0})}{\chi_{mm}(0, \mathbf{0}^+)}. \quad (7)$$

Here we used the fact that the difference between the q - and ω -limits of $\chi_{mm}(\omega, \mathbf{q})$ stems from the spectral contribution of the hydrodynamic mode. From the argument in Sec. 3, this ratio must be unity for the susceptibility of a conserved quantity, which can be confirmed explicitly.

We show the numerical result of R in Fig. 6. The ratio vanishes if the chiral CP or the TCP is approached from the symmetric phase, which means that the critical divergence is generated by the sigma mode without any contribution from the p-h mode. From the broken phase, on the other hand, we see the finite portion of the divergence comes from the p-h mode spectrum in the chiral critical transition — even in the $\mu = 0$ case. Approaching the TCP along the critical line, we see that the contribution from the p-h mode increases and eventually saturates the spectral sum (2).

First one may ask why the p-h mode gives no contribution in the sym-

metric phase. This is because that the chirality and helicity is the same for a massless quark and that the chirality flip in the scalar coupling requires the finite momentum transfer \mathbf{q} . In the broken phase, a massive quark with definite chirality has both helicity components, and therefore the p-h mode spectrum remains contributing to the susceptibility in the $\mathbf{q} \rightarrow \mathbf{0}$ limit.

Next we note that the mixing of this p-h spectrum in the susceptibility of ρ and s is possible in the broken phase through the coupling proportional to the condensate σ . This mixing gives rise to the finite gap of these susceptibilities across the *chiral* critical line. This fact implies that the p-h mode contribution must be of order of $1/\sigma^2 \rightarrow \infty$ in the scalar channel, to cancel the σ^2 factor from the coupling.

At the TCP approached from the broken phase with fixed μ , χ_{mm} diverges as $1/\sigma^4$ while $\chi_{\mu\mu}$ and χ_{TT} blow up as $1/\sigma^2$, which is easily confirmed within the Ginzburg–Landau approach. Only the p-h mode spectrum with hydrodynamic character can cause this divergence in the NJL model. The sigma meson mode in the NJL model provides the singularity of order $1/\sigma^2$ to χ_{mm} at the TCP approached from the broken phase. From the symmetric phase, where $\sigma \equiv 0$, there is no contribution from the p-h mode and the critical divergence at the TCP is completely provided by softening of the sigma meson. The $\chi_{\mu\mu}$ and χ_{TT} are finite there.

Along the critical line with finite quark masses $m \neq 0$, $\chi_{\mu\mu}$ and χ_{TT} as well as χ_{mm} diverge with the same exponent. Generally these divergence must come from softening of a hydrodynamic mode in the system because the baryon number and the energy are conserved quantities. We can prove this within the NJL model as well as the time-dependent GL approach.

6. Summary

We have seen that, unlike at the chiral CP, the ordering density at the CP with finite quark mass m is a linear combination of the scalar density, the baryon number density and the energy density, and that the susceptibilities of these density diverge there. Since the susceptibility of a conserved density solely comes from the hydrodynamic spectrum, the associated critical soft mode must be hydrodynamic. We identified the p-h mode in the NJL model as this critical mode. Recently it is explicitly argued that the dynamic universality class of this point is the same as the liquid–gas critical point^{11,12}.

Experimentally, it is worthwhile to study the fluctuation of the conserved densities.¹ The correct evolution equation for the correlation length must be hydrodynamic one, which is slower than the sigma like motion.

In this sense the growth of the correlation length in the heavy ion events passing by the CP acquires a renewed interest.¹³

Along the critical line in the phase space of $T-\mu-m$, we have studied the changeover of the associated soft mode from the sigma meson mode at the chiral CP to the p-h mode at the CP with $m \neq 0$. This shift occurs at the TCP, where the critical soft mode is different between the symmetric and broken phases. The dynamic classification of this TCP will be theoretically interesting.^{7,11,12}

There is a speculated phase diagram of QCD in the space of $T-\mu-m-m_s$,¹⁴ in which we see several critical lines and surfaces. It seems important to keep the hydrodynamic viewpoint in mind when we study these criticalities.

Acknowledgments

One (H.F.) of the authors is grateful for the warm hospitality extended to him by KIAS. This work is supported in part by the Grants-in-Aid for Scientific Research of Monbu-kagaku-sho (No. 13440067).

References

1. For review, M.A. Stephanov, "QCD phase diagram and the critical point," arXiv:hep-ph/0402115.
2. M. Stephanov, K. Rajagopal and E.V. Shuryak, Phys. Rev. Lett. **81**, 4816 (1998).
3. M. Stephanov, K. Rajagopal and E.V. Shuryak, Phys. Rev. D **60**, 114028 (1999).
4. I. Lawrie and S. Sarbach, in *Phase Transitions and Critical Phenomena*, ed. by C. Domb and J. Lebowitz (Academic Press, NY, 1984), Vol. 9, pp. 1.
5. T. Hatsuda and T. Kunihiro, Phys. Rev. Lett. **55**, 158 (1985).
6. H. Fujii, Phys. Rev. D **67**, 094018 (2003).
7. H. Fujii and M. Ohtani, arXiv:hep-ph/0401028; arXiv:hep-ph/0402263.
8. T. Hatsuda and T. Kunihiro, Phys. Rept. **247**, 221 (1994).
9. S.P. Klevansky Rev. Mod. Phys. **64**, 649 (1992).
10. F. Karsch, E. Laermann and C. Schmidt, Phys. Lett. B **520**, 41 (2001).
11. D.T. Son and M.A. Stephanov, arXiv:hep-ph/0401052.
12. P.C. Hohenberg and B.I. Halperin, Rev. Mod. Phys. **49**, 435 (1977).
13. B. Berdnikov and K. Rajagopal, Phys. Rev. D **61**, 105017 (2000).
14. C. Schmidt, C. R. Allton, S. Ejiri, S. J. Hands, O. Kaczmarek, F. Karsch and E. Laermann, Nucl. Phys. Proc. Suppl. **119**, 517 (2003).